AIAA 91-1596
Time Dependent Calculations Using Multigrid, with Applications to Unsteady Flows Past Airfoils and Wings

A. Jameson
Princeton University
Princeton, NJ

AIAA 10th Computational Fluid Dynamics Conference
June 24-26, 1991 / Honolulu, HI

137

Time Dependent Calculations Using Multigrid, with Applications to Unsteady Flows Past Airfoils and Wings

Antony Jameson
Princeton University
Department of Mechanical and Aerospace Engineering
Princeton, NJ 08544

1. INTRODUCTION

A major factor leading to the widespread acceptance of computational fluid dynamics in the design environment has been the steady and continuing reduction of computational costs, due both to improvements in computer hardware and to improvements in algorithms. The multigrid technique has proved to be a particularly effective method to reduce the costs of steady state calculations, both for potential flow models, and for solutions of the Euler and Navier Stokes Equations [ref. 1-3].

Time dependent calculations are needed for a variety of important applications, such as flutter analysis, or the analysis of the flow past a helicopter in forward flight. A comprehensive survey may be found in the review paper of Edwards and Thomas [ref. 4]. If an explicit scheme is used to calculate an unsteady flow, the permissible time step for stability of the scheme may be much smaller than that needed to attain reasonable accuracy, with the consequence that an excessively large number of time steps must be used. Implicit schemes allow much larger time steps, but the work required in each time step may become excessively large, especially in three dimensional calculations.

In this paper it is proposed to use a multigrid scheme as a driver for a fully implicit time stepping scheme. This may pay off, in particular for problems in which there are very large variations in mesh size, where the use of an explicit scheme would result in a very severe restriction on the time step, based on the smallest cells in the mesh. The method has been applied to both two and three dimensional unsteady flows past moving bodies. In order to allow the use of body fitted coordinates the Euler equations are formulated in a general moving coordinate system allowing for deformation as well as displacement of the mesh. Preliminary applications are to pitching airfoils and wings.

2. FORMULATION OF THE SCHEME

Let p, ρ, E, and H be the pressure, density, total energy, and total enthalpy of the fluid. Also let x_i be Cartesian coordinates and let u_i be the velocity components. The equations for inviscid flow can then be written, using the convention that repeated indices denote summation, as

$$\frac{\partial w}{\partial t} + \frac{\partial f_i(w)}{\partial x_i} = 0 \qquad (1)$$

where the vector of dependent variables is

$$w = \begin{bmatrix} \rho \\ \rho u_1 \\ \rho u_2 \\ \rho u_3 \\ \rho E \end{bmatrix} \qquad (2)$$

and the flux vectors are

$$f_i = \begin{bmatrix} \rho u_i \\ \rho u_1 u_i + p\delta_{1i} \\ \rho u_2 u_i + p\delta_{2i} \\ \rho u_3 u_i + p\delta_{3i} \\ \rho H u_i \end{bmatrix} \qquad (3)$$

Also

$$p = (\gamma - 1)\rho \left[E - \frac{u_i^2}{2} \right] \qquad (4)$$

and

$$\rho H = \rho E + p \qquad (5)$$

where γ is the ratio of specific heats. For a general body fitted moving coordinate system with coordinates X_i, let J be the determinant of the transformation

$$J = \left| \frac{\partial x}{\partial X} \right|$$

and suppose that the mesh is moving with local velocity components $umesh_i$.

The equations now become

$$\frac{\partial}{\partial t}(Jw) + \frac{\partial F_j}{\partial x_j} = 0 \qquad (6)$$

where

$$F_j = J \frac{\partial X_j}{\partial x_i}(f_i - umesh_i\ w) \qquad (7)$$

These may be written in integral form for a domain D with boundary B as

$$\frac{\partial}{\partial t} \int_D w dV + \int_B (f_i - umesh_i\ w)\ dS_i = 0 \qquad (8)$$

where dS_i is the component of area projected in the x_i direction.

A finite volume scheme is derived by applying (8) directly to control volumes to give a set of ordinary differential equations of the form

$$\frac{d}{dt}(wV) + R(w) = 0 \qquad (9)$$

where V is the cell volume, and the residual R(w) is evaluated by summing the fluxes $(f_i - umesh_i\ w)\ S_i$ through the cell faces.

In order to prevent the appearance of high frequency modes corresponding to odd and even point oscillations, and also to prevent oscillations in the neighborhood of shock waves, artificial dissipative terms are introduced to provide an upwind bias (ref 2, 3). The dissipative terms are constructed by adding dissipative fluxes at the point i,j,k of the form

$$d_{i+1/2,j,k} - d_{i-1/2,j,k} + d_{i,j+1/2,k}$$

$$- d_{i,j-1/2,k} + d_{i,j,k+1/2} - d_{i,j,k-1/2}$$

The dissipative flux between the points i,j,k and i + 1,j,k is typically a blend of first and third differences

$$d_{i+1/2,j,k} = \varepsilon^{(2)}\, R_{i+1/2,j,k}\, \Delta_{i+1/2,j,k}$$

$$- \varepsilon^{(4)}\, R_{i+1/2,j,k} \left[\Delta_{i+3/2,j,k} + \right.$$

$$\left. -2\Delta_{i+1/2,j,k} + \Delta_{i-1/2,j,k} \right]$$

where

$$\Delta_{i+1/2,j,k} = w_{i+1,j,k} - w_{i,j,k}$$

The coefficient $R_{i+1/2,j,k}$ can be the spectral radius of the Jacobian matrix corresponding to the flux through the face

$$A = \frac{\partial}{\partial w} (f_i - \text{umesh}_i\, w)\, S_i$$

or if A is decomposed by its eigenvectors as

$$A = T \Lambda T^{-1}$$

one may take

$$R = |A| = T\, |\Lambda|\, T^{-1}$$

The use of a matrix coefficient in this form corresponds to flux difference splitting (ref. 5-7), and then the choice $\varepsilon^{(2)} = 1$, $\varepsilon^{(4)} = 0$ gives a pure upwind scheme. To reduce the level of dissipation $\varepsilon^{(2)}$ is taken proportional to the normalized second difference of the pressure

$$\left| \frac{p_{i+1,j,k} - 2p_{i,j,k} + p_{i-1,j,k}}{p_{i+1,j,k} + 2p_{i,j,k} + p_{i-1,j,k}} \right|$$

while $\varepsilon^{(4)}$ is taken as the positive difference of a constant and $\varepsilon^{(2)}$

$$\varepsilon^{(4)} = \max \left[\left(K - \varepsilon^{(2)}\right), 0 \right]$$

such that near shock waves the higher differences are switched off to prevent oscillations. This corresponds to the use of flux limiters (ref 7). Alternatively flux limiters may be directly included (ref 5,6).

Multigrid time stepping schemes have been developed to solve the steady state equations very rapidly (ref. 2,3). These schemes sacrifice time accuracy to achieve fast convergence. A multigrid time stepping scheme can be formulated so that it approximates the true time dependent evolution of the system (ref 8), but the accuracy decreases as the number of grids is increased. An alternative, adopted here, is to use the multigrid scheme as a driver for a fully implicit time stepping scheme. Thus equation (9) is approximated as

$$D_t \left[w^{(n+1)}\, V^{(n+1)} \right] + R\left[w^{(n+1)} \right] = 0 \quad (10)$$

Here the time level $n\Delta t$ is denoted by the superscript n, V is the cell volume, and R(w) is the residual. Also D_t is a k^{th} order accurate backward difference operator of the form

$$D = \frac{1}{\Delta t} \sum_{q=1}^{k} \frac{1}{q} \left[\Delta^-\right]^q$$

where

$$\Delta^- w^{(n+1)} = w^{(n+1)} - w^{(n)}$$

In the current implementation a second order accurate difference operator is used, yielding the equation

$$\frac{3}{2\Delta t} \left[w^{n+1}\, V^{n+1} \right] - \frac{2}{\Delta t} \left[w^{n}\, V^{n} \right] +$$

$$\frac{1}{2\Delta t} \left[w^{n-1}\, V^{n-1} \right] + R\left[w^{n+1} \right] = 0 \quad (11)$$

Applied to a linear differential equation of the form

$$\frac{dw}{dt} = \alpha w$$

the second order backward difference scheme is A-stable (stable for all values of $\alpha\Delta t$ in the left half of the complex plane). It has been shown by Dahlquist and Jeltsch (ref. 9) that A-stable linear multistep schemes are not better than second order accurate. The trapezoidal scheme is A-stable with a smaller error constant, but is undamped as $|\alpha\Delta t|$ becomes very large. Consequently the second order backward difference scheme has been preferred for this work.

Equation (11) is now treated as a modified steady state problem to be solved by a multigrid scheme using variable local time steps in a fictitious time t^*:

$$\frac{\partial w}{\partial t^*} + R^*(w) = 0 \qquad (12)$$

where the modified residual $R^*(w)$ is defined as

$$R^*(w) = \frac{3}{2\Delta t} w + \frac{1}{V^{n+1}} \left[R(w) - S\left[w^{(n)}, w^{(n-1)} \right] \right] \qquad (13)$$

with the fixed source term

$$S\left[w^{(n)}, w^{(n-1)} \right] = \frac{2}{\Delta t} w^{(n)} V^{(n)} - \frac{1}{2\Delta t} w^{(n-1)} V^{(n-1)} \qquad (14)$$

The multigrid scheme is driven by a multistage time stepping scheme in t^*.

If one considers a linear model problem corresponding to equations (12-14), with a Fourier mode of the form $w = \hat{w} \exp(i\, p_j\, x_j)$, the term $\frac{3}{2\Delta t} w$ shifts the Fourier symbol to the left along the negative real axis. Thus the time stepping scheme should have a stability region which contains a substantial interval of the negative real axis as well as intervals along the imaginary axis. To achieve this it pays to treat the convective and dissipative terms in a distinct fashion. Thus the residual is split as

$$R^*(w) = Q(w) + D(w)$$

where $Q(w)$ is the convective part and $D(w)$ the dissipative part. Then the multistage time stepping scheme is formulated as

$$w^{(n+1,0)} = w^{(n)}$$

. . . .

$$w^{(n+1,k)} = w^{(n)} - \alpha_k \Delta t^* \left[Q^{(k-1)} + D^{(k-1)} \right]$$

. . . .

$$w^{(n+1)} = w^{(n+1,m)}$$

where $\alpha_m = 1$, and

$$Q^{(0)} = Q\left[w^{(n)} \right], \quad D^{(0)} = D\left[w^{(n)} \right]$$

. . . .

$$Q^{(k)} = Q\left[w^{(n+1,k)} \right]$$

$$D^{(k)} = \beta^{(k)} D\left[w^{(n+1,k)} \right] + (1 - \beta^{(k)}) D^{(k-1)}$$

The coefficients α_k are chosen to maximize the stability interval along the imaginary axis, and the coefficients β_k are chosen to increase the stability interval along the negative real axis.

Two schemes which have been found to be particularly effective are tabulated below. The first is a four-

stage scheme with two evaluations of dissipation. Its coefficients are

$$\alpha_1 = 1/3 \qquad \beta_1 = 1$$
$$\alpha_2 = 4/15 \qquad \beta_2 = 1/2$$
$$\alpha_3 = 5/9 \qquad \beta_3 = 0$$
$$\alpha_4 = 1 \qquad \beta_4 = 0$$

The second is a five-stage scheme with three evaluations of dissipation. Its coefficients are

$$\alpha_1 = 1/4 \qquad \beta_1 = 1$$
$$\alpha_2 = 1/6 \qquad \beta_2 = 0$$
$$\alpha_3 = 3/8 \qquad \beta_3 = .56$$
$$\alpha_4 = 1/2 \qquad \beta_4 = 0$$
$$\alpha_5 = 1 \qquad \beta_5 = .44$$

The multigrid scheme is a full approximation scheme defined as follows. Denote the grids by a superscript k. Start with a time step on the finest grid k = 1. Transfer the solution from a given grid to a coarser grid by a transfer operator $P_{k,k-1}$, so that the initial state on grid k is

$$w_k^{(0)} = P_{k,k-1}\, w_{k-1}$$

Then on grid k the time stepping scheme is reformulated as

$$w_k^{(q+1)} = w_k^{(0)} - \alpha_n \Delta t^* \left[R_k^*(q) + G_k\right]$$

where the forcing function G_k is defined as the difference between the aggregated residuals transferred from grid k-1 and the residual recalculated on grid k. Thus

$$G_k = Q_{k,k-1}\, R^*\left[w_{k-1}\right] - R^*\left[w_k^{(0)}\right]$$

where $Q_{k,k-1}$ is another transfer operator. On the first stage the forcing term G_k simply replaces the coarse grid residual by the aggregated fine grid residuals. Consequently the source term S in equation (13) can be omitted from the coarse grid residuals. The accumulated correction on a coarser grid is transferred to the next higher grid by an interpolation operator $I_{k-1,k}$ so that the solution on grid k-1 is updated by the formula

$$w_{k-1}^{new} = w_{k-1} + I_{k-1,k}\left[w_k - w_k^{(0)}\right]$$

The whole set of grids is traversed in a W cycle in which time steps are only performed when moving down the cycle.

3. RESULTS

The multigrid implicit scheme defined by equations (12-14) has been applied to both two and three dimensional flows. Reference 10 provides unsteady flow measurements for a test case in the flutter regime. This case, labelled AGARD CT-6, is a pitching NACA 64A010 airfoil at a Mach number of .796. The mean angle of attack is zero, the pitching amplitude is ±1.01 degrees, and the reduced frequency, defined as

$$k = \frac{\omega\, \text{chord}}{2q_\infty}$$

is 2.02. Calculations were performed on an O mesh with 160 x 32 cells (displayed in Figure 1), with 24 and 36 time steps per oscillation period. These gave essentially the same result. In both case 15 multigrid cycles were used in each implicit time step, giving an error reduction of two orders of magnitude or more. With 24 steps in each period the Courant number reached values as high as 4138 in the very small cells in the neighborhood of the trailing edge. Figure 2 shows the result obtained with 36 time steps per period. The pressure distribution is displayed at several values of the phase angle ωt during the second

period, with + symbols for the upper surface and x symbols for the lower surface. Figure 3 shows a comparison of the computed values of the lift coefficient versus the angle of attack with the measurements. These values lie on a slanting oval curve because of the phase lag between the lift and the angle of attack. The measurements shows a slightly smaller total variation of lift, and lie on a slightly broader oval. The discrepancy is extremely similar to the discrepancy which was found when the same case was calculated using an explicit multistage scheme on a C-mesh (ref 6), suggesting that it may be attributed to viscous effects.

In order to test the three dimensional scheme calculations have been performed for the ONERA M6 wing with a 96 x 16 x 24 C-mesh. Figure 4 shows the result for an unsteady flow at Mach .840 over a pitching wing. In this case the reduced frequency is .1, and the amplitude is ± 5 degrees about a mean angle of attack of zero degrees. The figure displays the pressure distribution at the root and mid-span stations Z = 0 and Z = .5 over one complete oscillation period, at phase intervals of 90 degrees, with + symbols for the upper surface and x symbols for the lower surface. The maximum Courant number in this calculation exceeded 950, and 15 multigrid cycles were again found to give a sufficient error reduction in each step. In general one may expect there to be a trade-off between the step size and the number of multigrid cycles needed for convergence of the implicit equations.

4. CONCLUSION

Preliminary trials confirm that the multigrid implicit scheme can be used to calculate unsteady flows in the flutter regime with 24 to 36 time steps in each oscillation period, corresponding to Courant numbers larger than 4000 in the smallest mesh cells. Direct use of an explicit multistage scheme with residual averaging allows Courant numbers in the range of 5 to 8 to be attained (ref. 6). Assuming the use of 10 to 15 multigrid cycles in each implicit time step, the multigrid implicit scheme will show a pay off in reduced computational costs, as long as sufficient accuracy can be realized while using time steps corresponding to Courant numbers of 200 or more. In situations allowing the use of Courant numbers in the range of 10 to 100, one might prefer to use a time accurate multistage multigrid scheme with a tau correction to reduce the errors introduced by the coarse grids (ref 11). In order to provide optimal efficiency for a range of problems, one may incorporate in a single computer program the three options of a single grid multistage scheme, a multigrid multistage scheme, and a multigrid implicit scheme of the type proposed in this paper. Ultimately one could introduce an adaptive scheme to select different options in different zones depending on the local situation.

It appears that a computationally efficient algorithm for unsteady flows could offer significant benefits in a variety of applications. These include helicopter rotors in forward flight [ref. 12,13], counter rotating propfans [ref. 14], rotor-stator combinations in turbomachinery [ref. 15-16], aeroelastic problems, oscillatory flows induced by viscous effects, and the calculation of acoustic signatures. A computer program to treat helicopter rotors by the present method is currently under development. This incorporates a multi-sectored rotating mesh with one blade in each sector, and mesh deformation to allow for blade flapping. A second anticipated extension is to wing flutter calculations. Bendiksen and Kousen used the program of Venkatakrishnan and Jameson [ref. 6] to study a two dimensional flutter model, and discovered limit cycles due to nonlinear

transonic effects [ref. 17-18]. With the new implicit program there is now an opportunity to explore similar effects in three dimensional flow.

5. REFERENCES

1. R. H. Ni "A Multiple Grid Scheme for Solving the Euler Equations," AIAA Journal, Vol. 20, 1982, pp. 1565-1571.

2. A. Jameson, "Solution of the Euler Equations by a Multigrid Method," Applied Math. and Computation, Vol. 13, 1983, pp. 327-356.

3. A. Jameson, "Multigrid Algorithms for Compressible Flow Calculations," Proceedings of the Second European Conference on Multigrid Methods, Cologne, 1985, edited by W. Hackbusch and U. Trottenburg, Lecture Notes in Mathematics, Vol. 1127, Springer Verlag, 1986, pp. 166-201.

4. J. W. Edwards and J. L. Thomas, "Computational Methods for Unsteady Transonic Flows," AIAA Paper 86-0107, AIAA 25th Aerospace Sciences Conference, Reno, 1987.

5. A. Jameson, "A Non-Oscillatory Shock Capturing Scheme Using Flux Limited Dissipation," Princeton University Report MAE 1653, 1984, in Large Scale Computations in Fluid Mechanics, edited by B. E. Engquist, S. Osher, and R.C. J.Sommerville, Lecture Notes in Applied Mathematics, Vol. 22, Part 1, AMS, 1985, pp. 345-370.

6. V. Venkatakrishnan and A. Jameson, "Computation of Unsteady Transonic Flows by Solution of the Euler Equations," AIAA Journal, Vol. 26, 1988, pp. 974-981.

7. R. C. Swanson and E. Turkel, "On Central-Difference and Upwind Schemes," ICASE Report 90-44, 1990.

8. D. C. Jespersen, "A Time-Accurate Multiple-Grid Algorithm," AIAA Paper 85-1493, Proceedings AIAA 7th Computational Fluid Dynamics Conference, Cincinnati, 1985, pp. 58-66.

9. R. Jeltsch, "Stability on the Imaginary Axis and A Stability of Linear Multistep Methods," BIT, Vol. 18, 1978, pp. 170-174.

10. S. S. Davis, "NACA 64AO10, Oscillatory Pitching," Compendium of Unsteady Aerodynamic Measurements, AGARD Report 702, 1982.

11. M. Meinke and D. Hänel, "Time Accurate Multigrid Solutions of the Navier Stokes Equations," presented at the Third European Conference on Multigrid Methods, Bonn, 1990.

12. B. E. Wake, L. N. Sankar and S. G. Lekoudis, "Computation of Rotor Blade Flows Using the Euler Equations," J. of Aircraft, Vol. 23, 1986, pp. 582-588.

13. B. E. Wake and L. N. Sankar, "Solutions of the Navier-Stokes Equations for the Flow About a Rotor Blade," J. American Helicopter Society, Vol. 34, 1989, pp. 13-23.

14. D. L. Whitfield, T. W. Swafford, J. M. Janus, R. A. Mulac and D. M. Belk, "Three-Dimensional Unsteady Euler Solutions for Propfans and Counter-Rotating Propfans in Transonic Flow," AIAA Paper 87-1197, AIAA 19th Fluid Dynamics, Plasma Dynamics and Lasers Conference, Honolulu, 1987.

15. M. M. Rai, "Navier-Stokes Simulations of Rotor/Stator Interaction Using Patched and Overlaid Grids," J. Propulsion, Vo. 3, 1987, pp. 387-396.

16. M. B. Giles, "Calculation of Unsteady Wake/Rotor Interaction," J. Propulsion, Vol. 4, 1988, pp. 356-362.

17. O. O. Bendiksen and K. A. Kousen, "Transonic Flutter Analysis Using the Euler Equations," AIAA Paper 87-0911, AIAA Dynamics Specialists Conference, Monterey, 1987.

18. K. A. Kousen and O. O. Bendiksen, "Nonlinear Aspects of the Transonic Aeroelastic Stability Problem," AIAA Paper 88-2306, AIAA/ASME/ASCE/AHS 29th Structures, Structural Dynamics and Materials Conference, Williamsburg, 1988.

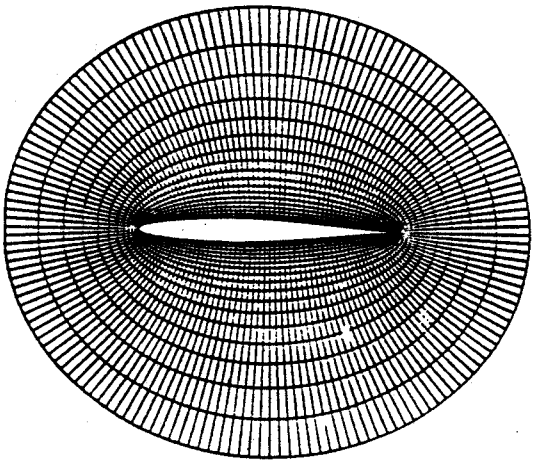

Figure 1

Inner part of the 160 x 32 O mesh for the NACA 64A010 airfoil

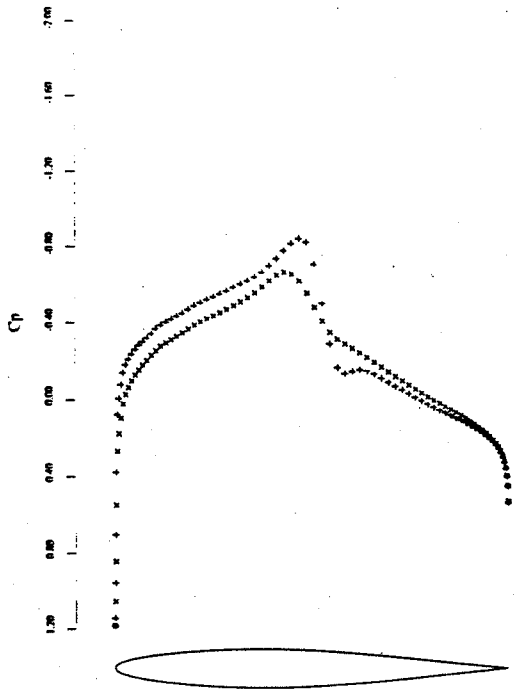

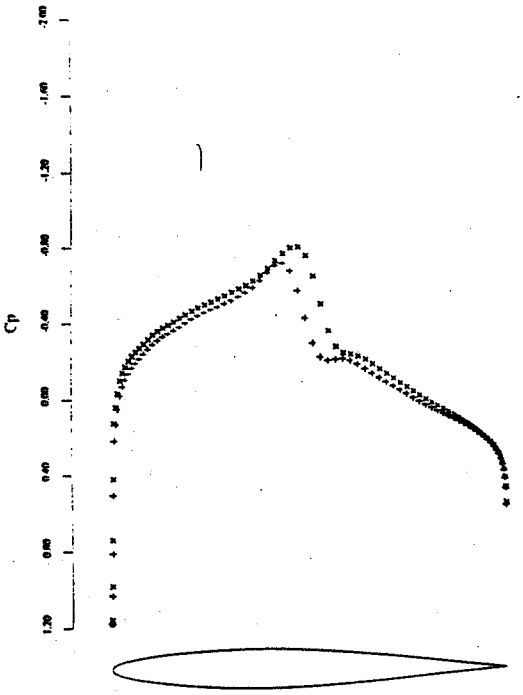

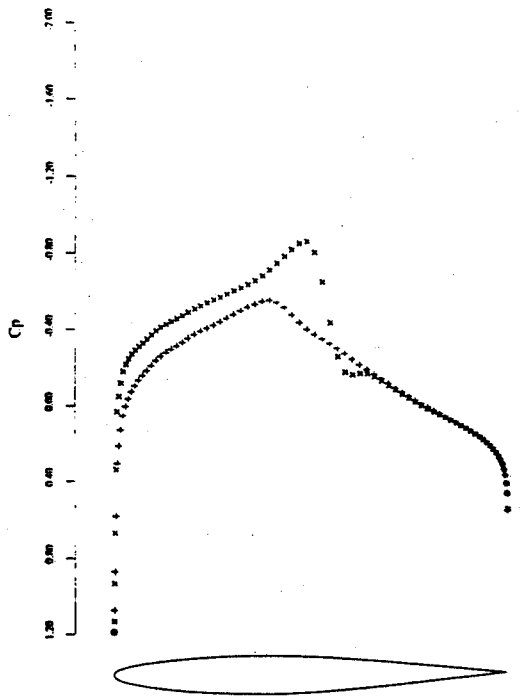

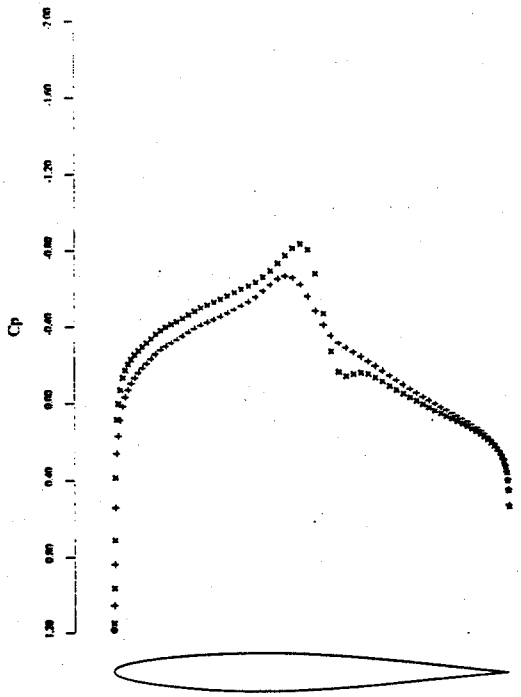

Figure 2

Pressure Distribution over the NACA 64A410
at different phase angles during the oscillation period

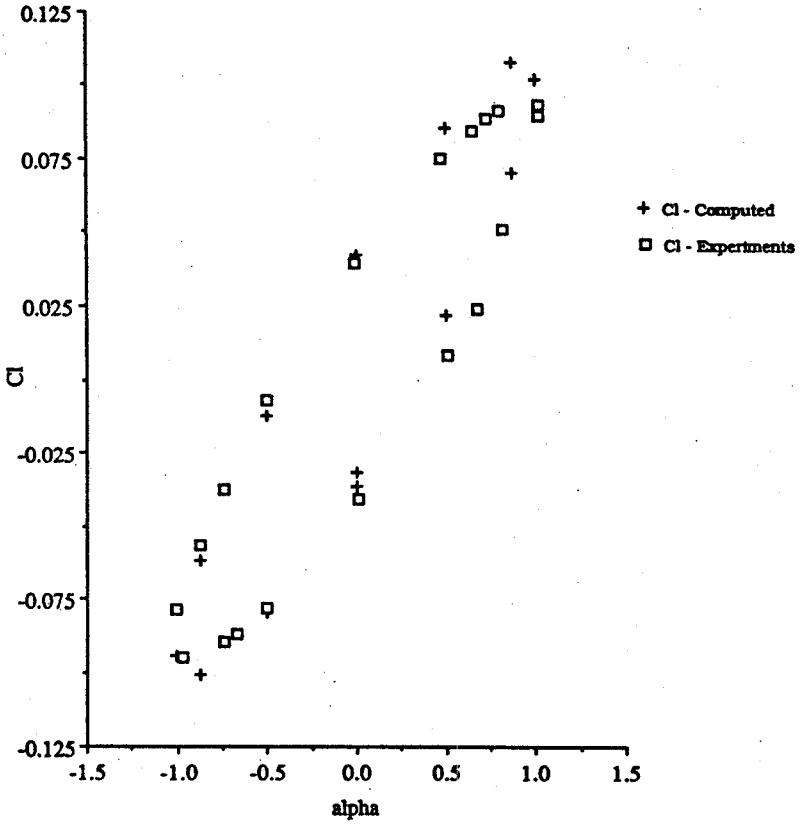

Figure 3

Comparison of computed and measured variation of the lift coefficient of the NACA 64A010 airfoil during a oscillation period

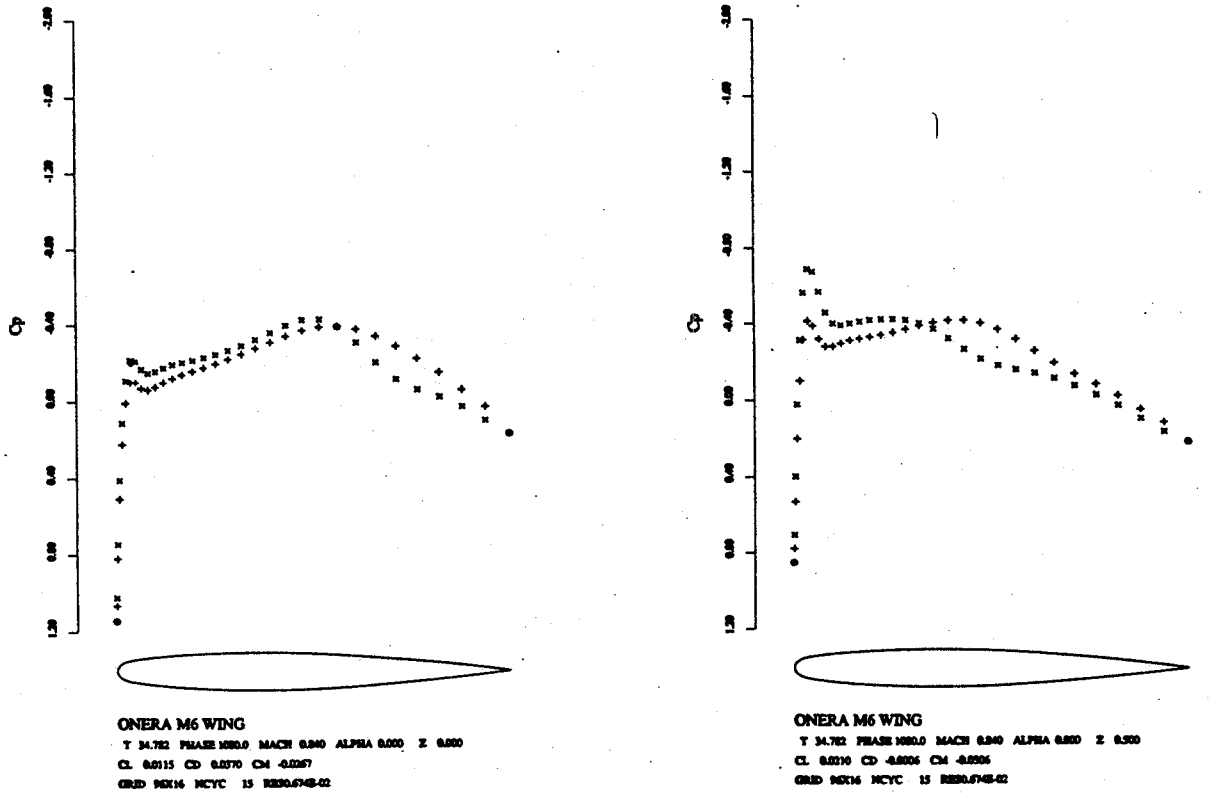

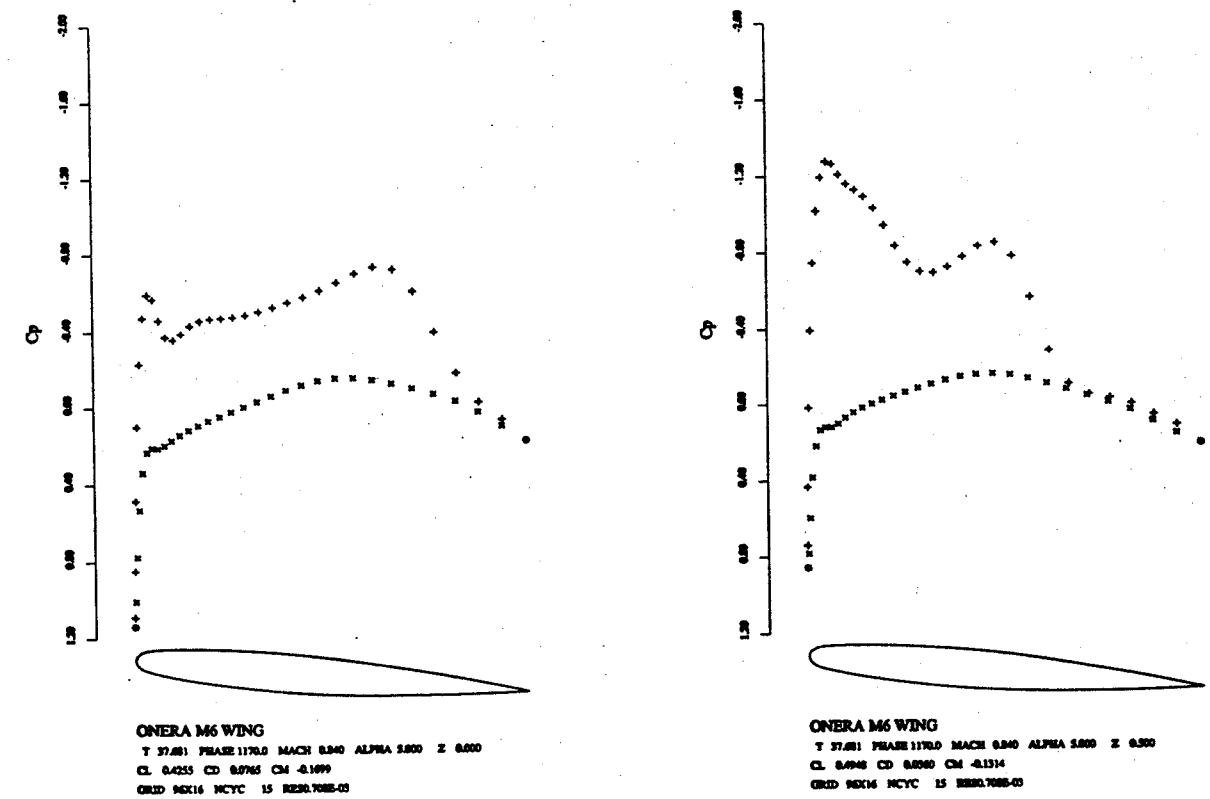

Figure 4

Pressure distribution at the midspan over the ONERA M6 wing at different phase angles during the oscillation period

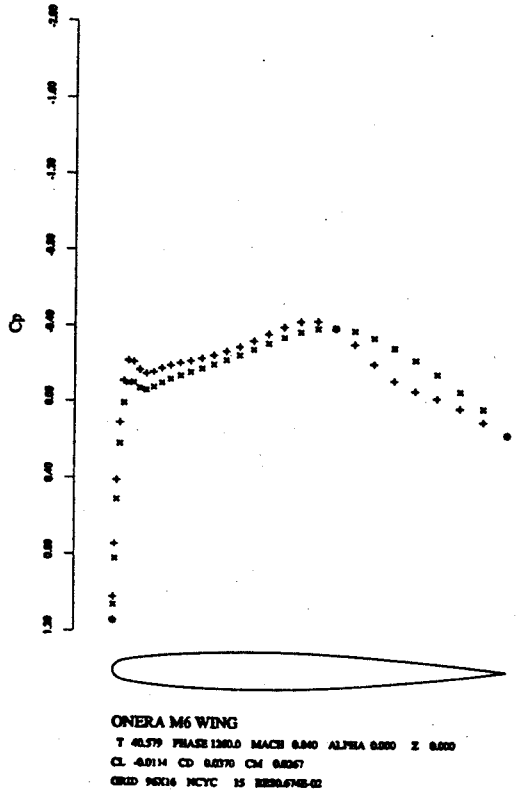

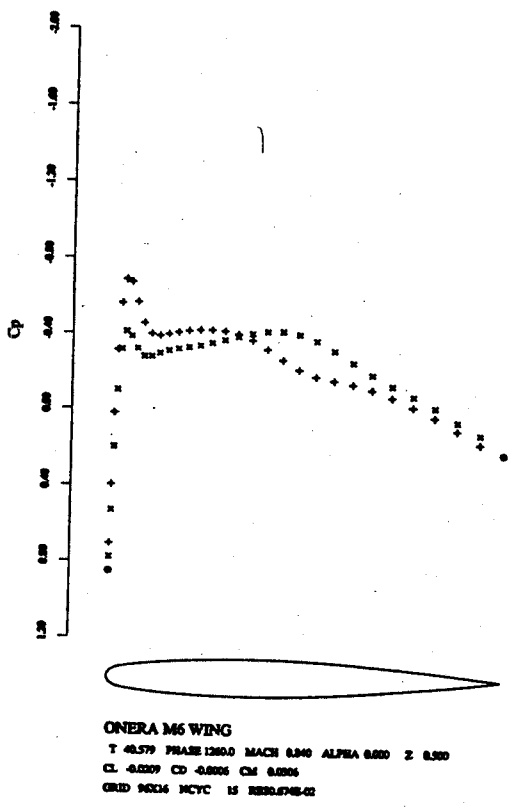

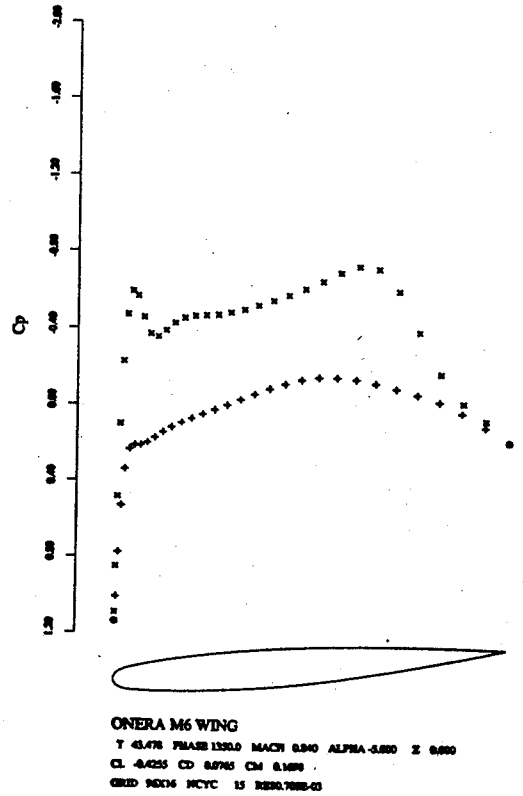

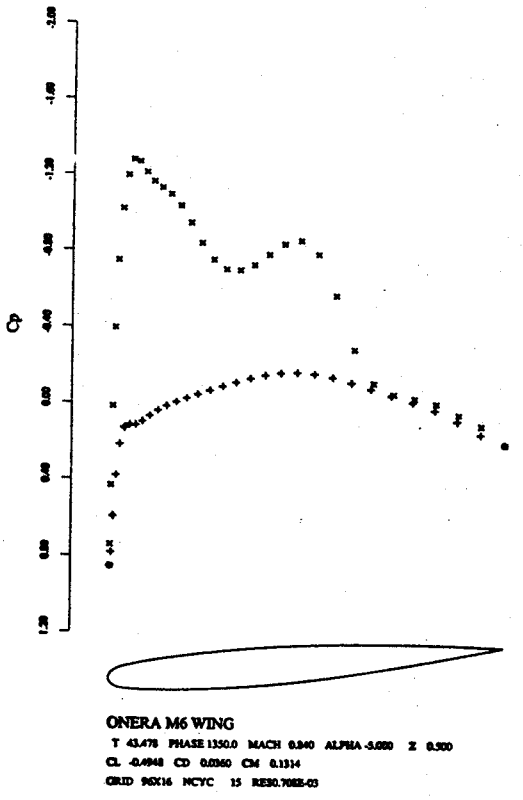

Figure 4 (Continued)

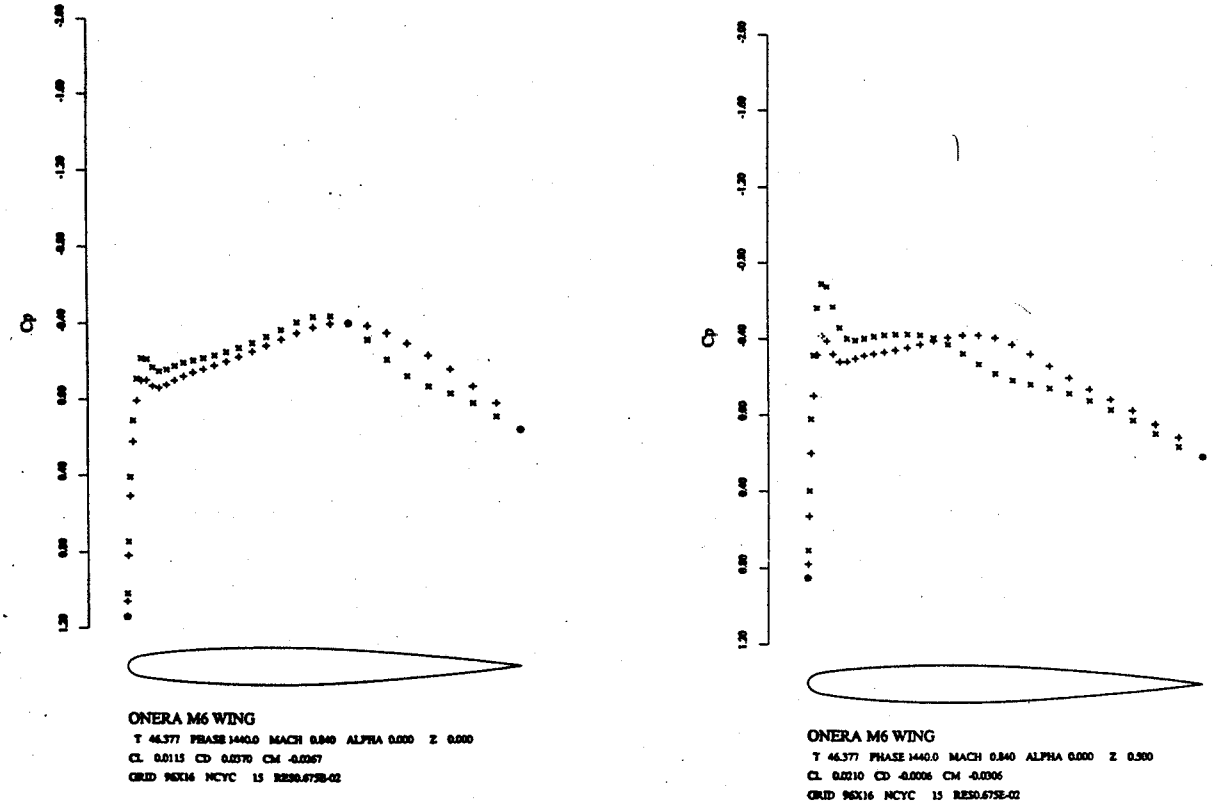

Figure 4 (Concluded)